Quaternary Science Reviews 168 (2017) 182–193

Contents lists available at ScienceDirect

Quaternary Science Reviews

journal homepage: www.elsevier.com/locate/quascirev

Holocene evolution of Hans Tausen Iskappe (Greenland) and implications for the palaeoclimatic evolution of the high Arctic

Harry Zekollari [a, b, *], Benoit S. Lecavalier [c], Philippe Huybrechts [a]

[a] Earth System Science & Department Geografie, Vrije Universiteit Brussel, Brussels, Belgium
[b] Laboratory of Hydraulics, Hydrology and Glaciology (VAW), ETH Zürich, Zurich, Switzerland
[c] Department of Physics and Physical Oceanography, Memorial University, St. John's, Newfoundland, Canada

ARTICLE INFO

Article history:
Received 6 March 2017
Received in revised form
8 May 2017
Accepted 12 May 2017

Keywords:
Holocene
Glaciology
Greenland
Ice core
Ice cap
Numerical modelling
3-D Ice Flow model
High Arctic
Palaeoclimate
Hans Tausen Iskappe

ABSTRACT

In this study the Holocene evolution of Hans Tausen Iskappe (Peary Land, North Greenland) is investigated. Constraints on the ice cap evolution are combined with climatic records in a numerical ice flow – surface mass balance (SMB) model to better understand the palaeoenvironmental and climatic evolution of this region. Our simulations suggest that after disconnecting from the Greenland Ice Sheet (GrIS) the ice cap had roughly its present-day size and geometry around 9–8.5 ka BP. During the Holocene Thermal Maximum (HTM) the southern part of the ice cap is modelled to collapse, while the northern part of the ice cap survived this warmer period. The late Holocene regrowth of the ice cap to its maximum Neoglacial extent at the end of the Little Ice Age (LIA) can be reproduced from the temperature reconstruction. The simulations suggest that over the last millennia the local precipitation may have been up to 70–80% higher than at present. By coupling the pre-industrial temperature forcing to a post-LIA warming trend, it is suggested that the warming between the end of the LIA and the period 1961–1990 was between 1 and 2 °C. In all experiments the ice flow model complexity and horizontal resolution have only a minor effect on the long-term evolution of the ice cap. We further conclude that the glacial isostatic adjustment has a significant effect on the modelled Holocene ice cap evolution. This suggests that modelling studies of millennial-scale ice cap evolution should focus on SMB and boundary conditions, rather than on complex ice dynamics.

1. Introduction

Holocene fluctuations of the glaciers and ice caps (GICs) that surround the Greenland ice sheet (GrIS) are poorly understood, as only few measurements exist to constrain their evolution (Kelly and Lowell, 2009). To address this lack of data and to obtain a better insight in the Holocene evolution of Greenlandic GICs, modelling studies are a powerful tool. Such studies improve our understanding of the role of past changes on the present-day evolution of GICs (e.g. Gilbert et al., 2016). They also allow us to constrain palaeoclimatic conditions, by comparing modelled past changes in ice masses with palaoglaciological inferences (e.g. Huybrechts, 1990; Pollard and DeConto, 2009; Steig et al., 2015; Goelzer et al., 2016). Furthermore a better understanding on the evolution of Greenlandic GICs and climatic conditions during the early and mid Holocene, when temperatures were higher than today, is of large interest, as this could provide information about changes to come in the future (cf. Masson-Delmotte et al., 2013). Of particular interest is the influence that a palaeo ice-free ocean may have had on the northern Greenland precipitation. This could provide insights in future precipitation increases following from the projected disappearance of the permanent Arctic ocean sea-ice in the coming decades (Singarayer et al., 2006; Collins et al., 2013; Overland and Wang, 2013).

Despite their importance, to our knowledge, no detailed modelling attempts exist to simulate the Holocene evolution of a local Greenlandic ice cap combining palaeoclimatic and palaeoglaciological constraints. In this study, we aim to solve for this lack of research by simulating the Holocene evolution of Hans Tausen Iskappe (Peary Land, see Fig. 1). A palaeomodelling study on this ice cap offers a number of unique opportunities:

* Corresponding author. Earth System Science & Department Geografie, Vrije Universiteit Brussel, Brussels, Belgium.
E-mail address: harry.zekollari@vub.be (H. Zekollari).

http://dx.doi.org/10.1016/j.quascirev.2017.05.010
0277-3791/

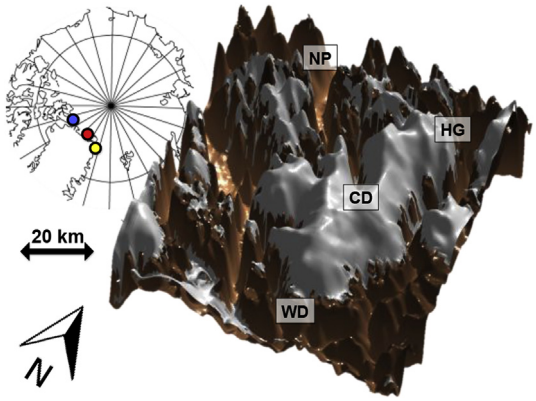

Fig. 1. Present-day geometry of Hans Tausen Iskappe (CD = Central Dome, HG = Hare Glacier, NP = Nord Passet, WD = Wandel Dal) (figure created with TopoZeko toolbox (Zekollari, 2016)). The inset shows the location of Hans Tausen Iskappe (red dot), the Agassiz ice cap (blue dot) and Flade Isblink (yellow dot). (For interpretation of the references to colour in this figure legend, the reader is referred to the web version of this article.)

(i) Despite its extreme northern location and remoteness a substantial wealth of field data exists for the present-day Hans Tausen Iskappe (Hammer, 2001). These data were previously used to extensively calibrate and validate a coupled ice flow – surface mass balance (SMB) model (Zekollari et al., 2017). The ice cap dynamics and sensitivity to climatic changes are therefore quite well understood.

(ii) A recently updated palaeotemperature record from the nearby Agassiz ice cap is available, spanning the past 12,000 years (Lecavalier et al., 2017). The proximity of the record is relatively unique. For Holocene palaeoglaciological modelling studies usually records from more distant locations (e.g. NGRIP) need to be used, which can be up to thousands of kilometres away from the site location and situated at a significantly higher elevation (e.g. Flowers et al., 2008).

(iii) There are several constraints on the past ice cap evolution, such as deglaciation dates and information from an ice core that was drilled to the bedrock (Clausen et al., 2001; Hammer et al., 2001; Landvik et al., 2001; Madsen and Thorsteinsson, 2001; Weidick, 2001). Present-day simulations suggest that the ice cap is highly sensitive to changes in climatic conditions, making constraints on its past evolution well suited to constrain past climatic changes.

We start by shortly reviewing the literature on the past evolution of the ice cap and its surroundings (section 2) and then describe the model (section 3) and the experimental setup (section 4). Subsequently the Holocene evolution of the ice cap is modelled (section 5). The implications and uncertainties of this modelling, both from a modelling perspective as from a palaeoclimatic perspective, are discussed in section 6.

2. Past evolution and present-day ice cap geometry

Glacial-geological data suggest that during the Last Glacial Maximum (LGM) the Hans Tausen Iskappe was a semi-independent ice cap, usually referred to as 'North Cap', which was connected to the GrIS (Bennike, 1987; Landvik et al., 2001; Larsen et al., 2010; Jakobsson et al., 2014). At that time it is believed that the GrIS and North Cap had shelf-based ice, which was likely controlled by very thick sea ice that prevented it from breaking up (Larsen et al., 2010; Jakobsson et al., 2014). Palaeorecords suggest that this shelf-based ice began to retreat around ca. 16 ka BP, before eventually breaking up around 10 ka BP in response to higher temperatures and an increased inflow of warm water through the Fram Strait (Larsen et al., 2010). Subsequently the ice margin in Peary Land started retreating (Bennike and Björck, 2002; Nørgaard-Pedersen et al., 2008; Larsen et al., 2010), a bit later than for other northern Greenland coastal areas, where the retreat typically started around 12.5–11.5 cal ka BP (Bennike and Björck, 2002; Funder et al., 2011b). During this retreat several short-lived re-advance episodes of local glaciers may have occurred (Funder et al., 2004; Möller et al., 2010; Larsen et al., 2015), as is also believed to be the case for other Greenlandic GICs (e.g. Ingólfsson et al., 1990).

After its disconnection from the GrIS it is believed that the ice cap had roughly its present-day extent sometime between 9 and 6 ka BP (Landvik et al., 2001). The lower bound (9 ka BP) corresponds to the earliest times when other northern Greenland ice masses reached their present-day position, as was for instance the case at Independence fjord (Bennike, 1987; Bennike and Weidick, 1999). Shells dated up to 8120 cal BP suggest that the area north of the present-day ice cap (Nordpasset, see Fig. 1) deglaciated before this time (Landvik et al., 2001). In the Wandel Dal, south of the present-day ice cap (Fig. 1), records suggest that the disconnection with the GrIS occurred somewhat later, potentially as late as 6 ka BP (Landvik et al., 2001).

The mass loss over Hans Tausen Iskappe persisted for several millennia, and in the mid-Holocene the ice cap was smaller than at present. Palaeorecords suggest that the ice cap may have (partly) disappeared (Madsen and Thorsteinsson, 2001). Crystal size analyses from an ice core drilled to the bed at the present-day Central Dome of Hans Tausen Iskappe (Madsen and Thorsteinsson, 2001) have been interpreted as indicating that the ice cap disappeared. The oldest ice was estimated to be 3.5 to 4.0 ka old and simple temperature calculations show that bottom temperatures were never near the melting point (Madsen and Thorsteinsson, 2001), meaning that the ice core should contain a preserved section since the time that the location was covered by the ice cap. Over the last millennia the ice cap grew and terminal moraines suggest that the maximum Neoglacial extent occurred at the end of the LIA, around 1900 AD (Landvik et al., 2001; Weidick, 2001). This is in line with most other GICs in Greenland (Kelly and Lowell, 2009; Balascio et al., 2015; Schweinsberg et al., 2017). During the first part of the 20th century the ice cap margin slightly retreated (Davies and Krinsley, 1962). The latter half of the 20th century was characterized by slower recession (limited to tens of meters), stand-still or even slight readvances (Weidick, 2001). The present-day ice cap volume is around 770 km^3 and locally the ice thickness reaches up to 600 m (Starzer and Reeh, 2001) (see Fig. 2 and Zekollari et al. (2017) for a more detailed account). It covers a higher-lying northern plateau (typically at 800–1100 m a.s.l.) and a lower-lying southern plateau (600–900 m a.s.l.). Except for a few neighbouring small ice masses (<300 km^2) (Weidick, 2001), at present the Hans Tausen Iskappe is the world's northernmost ice cap.

3. Ice flow – surface mass balance model

The Holocene evolution of the ice cap is simulated with a 3-D coupled ice flow –SMB model that was tuned and validated with present-day observations (Zekollari et al., 2017). The ice flow is calculated from a 3-D higher-order (HO) thermo-mechanical model (Fürst et al., 2011; Zekollari et al., 2013, 2014; Zekollari and Huybrechts, 2015) that is run at a 250-m horizontal resolution, with 21 vertical layers. The internal deformation is described through Nye's generalisation of Glen's flow law (Glen, 1955; Nye, 1957). A full 3-D calculation of the ice temperature is performed, accounting for diffusion, advection and basal heating (cf. Huybrechts, 1996). Surface temperatures are derived from the

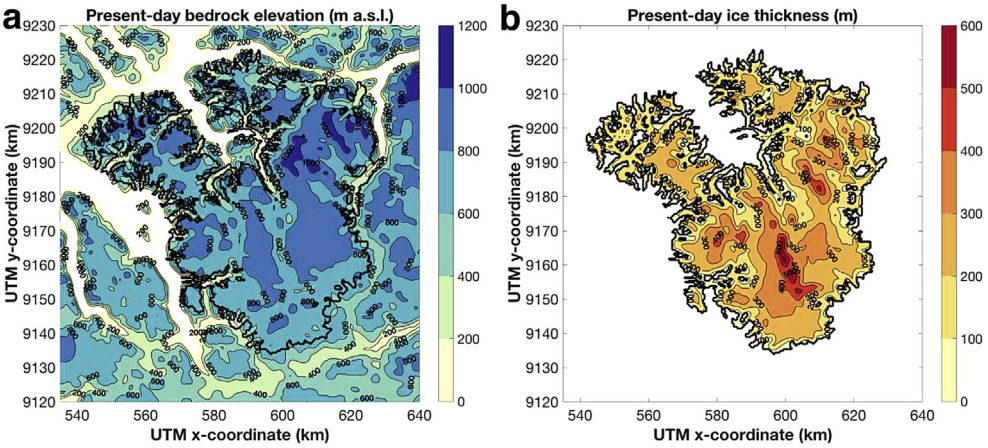

Fig. 2. Present-day (a) bedrock elevation and (b) ice thickness of Hans Tausen Iskappe (Starzer and Reeh, 2001).

mean annual temperature and a heating component related to refreezing, set at 20 K/m i.e. based on field observations (Reeh et al., 2001). The SMB is calculated from a positive degree-day (PDD) runoff/retention model (Janssens and Huybrechts, 2000). In this model melt rates are proportional to the PDD sum from monthly air temperatures assuming a variability of daily near-surface (2 m) temperatures around the monthly mean. Melt water storage and superimposed ice formation are incorporated. Precipitation is calculated from the regional climate model RACMO2.3, that was run for the present-day (Noël et al., 2016). The obtained average 1961–1990 field is scaled over time with a multiplication factor that depends on temperature and sea-ice conditions (see section 4.3. for details). This approach assumes that the precipitation pattern does not change over time. That is believed to be a reasonable assumption given that the precipitation pattern is mainly driven by the distance to the ocean and a shielding effect from the northern plateau of the ice cap, both of which do not change significantly over the Holocene. For a more detailed account on the ice flow - SMB model setup please refer to Zekollari et al. (2017).

4. Experimental setup

4.1. Initial conditions

The model spin-up requires careful consideration, as it may have a substantial influence on the Holocene evolution of the ice cap. The early Holocene evolution of the ice cap, when the ice mass disconnected from the GrIS, cannot explicitly be modelled. To this purpose a full Greenland model run over longer timescales would be needed (e.g. Huybrechts et al., 2011; Lecavalier et al., 2014). But even with a setup that encompasses the evolution of the GrIS, the exact timing and correct magnitude of the ice mass evolution over the present-day ice cap domain would most likely not be correctly reproduced given the small spatial scale of this domain in the larger Greenland context. Attempts were undertaken to produce a large early Holocene ice mass connected to the GrIS over the Hans Tausen domain as a starting point, but artefacts related to ice leaving the model domain and rectangular boundaries intersecting adjacent ice caps inhibited this. We therefore opt to start the simulations somewhat later in time, at selected moments between 9 and 6 ka BP, when the ice cap is believed to have had a roughly similar geometry as the present-day ice cap (see section 2). The starting point for the simulations is the 1961–1990 steady state geometry, which is close to the observed present-day ice cap (Zekollari et al., 2017). Experiments starting from the observed geometry (from 1995) and geometries based on colder ice (i.e. a stiffer, thicker ice cap) were also performed and indicated that the initial geometric conditions have a very limited effect on the Holocene ice cap evolution (not shown here).

4.2. Temperature forcing

4.2.1. Holocene (until 1850 AD)

A continuous temperature record is needed to simulate the Holocene evolution of the ice cap. A local ice core was drilled to the bed at the present-day Central Dome of Hans Tausen Iskappe (Clausen et al., 2001; Hvidberg et al., 2001; see Fig. 1), but it is not possible to directly derive a temperature series from this core based on either $\delta^{18}O$ or δD. This is in part due to the presence of many melt-layers that strongly disturbs the isotopic signal (Madsen and Thorsteinsson, 2001). Furthermore local surface elevation changes, which introduce a non-climatic bias, are unknown. These local elevation changes do not only result from changes in the ice cap geometry, but are also a consequence of bedrock changes as a result of glacial isostatic adjustments (GIA). Another non-climatic factor that can alter the $\delta^{18}O/\delta D$ signal is a change in the isotopic source, which can occur if the source region strongly changes (Lecavalier et al., 2013).

Instead, we use a recently revised temperature forcing that was derived from an ice core drilled on the Agassiz ice cap (Ellesmere Island, Canada) (Lecavalier et al., 2017). The Agassiz ice cap is situated at about the same latitude as the Hans Tausen ice cap, 400 km to the west (see Fig. 1). From a Greenlandic Holocene palaeorecord perspective this is relatively close, as for GrIS palaeomodelling studies a uniform temperature forcing is typically used from a deep drill site, which can be up to more than 1500 km away (e.g. Huybrechts, 2002; Lecavalier et al., 2014). The temperature forcing was corrected for a local elevation change signal as well as an isotopic signal related to a changing Innuitian Ice Sheet (IIS) (see Lecavalier et al. (2013, 2017) for a more detailed account). In this reconstruction a distinct HTM peak (Kaufman et al., 2004) occurs around 10.0–10.5 ka BP, after which a long-term cooling trend is initiated that lasts until 1850, approximately corresponding to the end of the LIA (Fig. 3a).

The updated Agassiz temperature reconstruction fits in the larger Greenland picture and is in agreement with palaeorecords from the vicinity of the Hans Tausen Iskappe. The reconstructed HTM peak, which follows a peak in precessional forcing around 12–10 ka BP (Berger and Loutre, 1991), occurs earlier than in a previous study where the effect of the IIS was neglected (Vinther

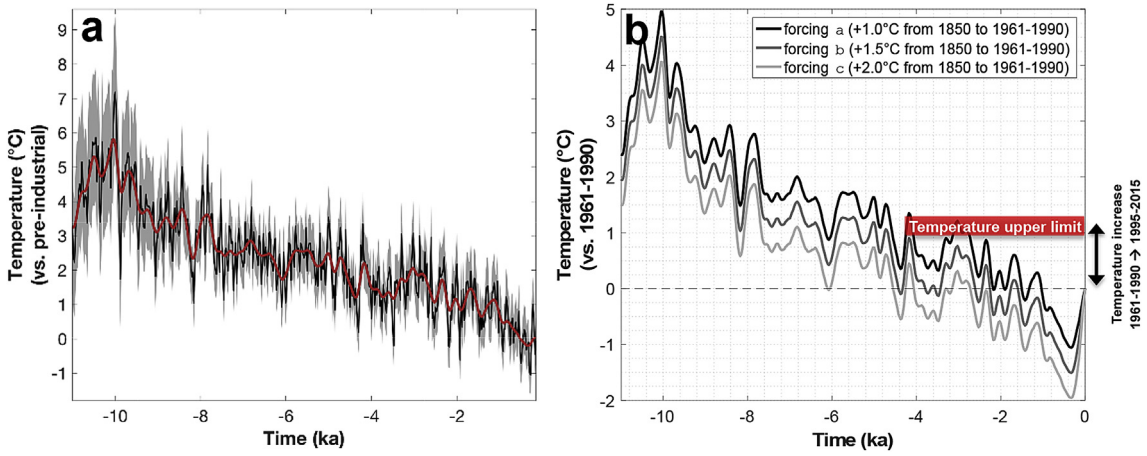

Fig. 3. (a) Pre-industrial forcing (from 11 ka BP until 1850), obtained from a recently revised ice-core record for the Agassiz ice cap (Lecavalier et al., 2017). The shaded area corresponds to the 2σ uncertainty, while the red line corresponds to the Gaussian filtered temperature record (σ = 75 year). (b) Different temperature histories (Gaussian filter, σ = 75 year) considered in this study, where the forcing until 1850 corresponds to the series shown in *a* and the post-1850 forcing is a linear increasing temperature trend of respectively 1.0 °C (forcing *a*), 1.5 °C (forcing *b*) and 2.0 °C (forcing *c*) between 1850 and 1961–1990. The red box illustrates the palaeorecord constraint that present-day (1995–2015) temperatures are unprecedented in the past 4 millennia. The 1995–2015 temperatures are about 0.9–1.2 °C warmer than 1961–1990 temperatures based on RACMO2.3 output (Noël et al., 2016). In both panels (a & b) the time is relative to 1961–1990. (For interpretation of the references to colour in this figure legend, the reader is referred to the web version of this article.)

et al., 2009). The updated timing of the HTM peak, at 10.5–10.0 ka BP, is now in line with the Agassiz ice core melt record (Fisher and Koerner, 2003; Fisher et al., 2012). Furthermore the updated timing matches with the timing of the ice-shelf break up in Peary Land at 10 ka BP (Larsen et al., 2010) and the concurrent transition from lacustrine to marine conditions for the nearby Bliss lake (100 km away) (Olsen et al., 2012). The magnitude of the HTM peak, 5.8 °C relative to pre-industrial after applying a 75-yr Gaussian filter (see Fig. 3b), is however more pronounced compared to the earlier reconstruction by Vinther et al. (2009). This peak magnitude agrees well with coupled modelling results, which suggest that due to a larger orbitally-forced insolation signal the warmest HTM conditions were found at high latitudes, where they reached around 5 °C above the pre-industrial level (Renssen et al., 2012). The magnitude is also in accordance with the average Greenland and Arctic Canada cooling of 3 °C between the HTM and the LIA (Briner et al., 2016), as an above-average HTM temperature peak is expected at high latitudes (Renssen et al., 2012).

For the early Holocene, when the IIS was still large (Simon et al., 2015), differences between the Agassiz temperature reconstruction between the studies by Vinther et al. (2009) and Lecavalier et al. (2017) are pronounced, but from 8 ka BP onwards both reconstructions are very similar. After the HTM, a long-term cooling trend started as a result of a decreasing orbitally-driven summer insolation, with positive feedbacks from ice and snow albedo (Otto-Bliesner et al., 2006). This Neoglacial cooling persisted until the end of the pre-industrial era. The late Holocene cooling in northern Greenland is supported by nearby lake and bog deposit records (Funder and Abrahamsen, 1988). Additional evidence comes from a high-resolution 3.5 ka palaeolimnological record for the nearby Kaffeklubben Sø lake, where microfossils suggest that the temperatures between 3.5 and 2.4 ka BP were warmer than between 2.4 ka BP and the LIA (Perren et al., 2012). Finally the decrease in melt-layers over the last 2-3ka in the Central Dome ice core also suggests a late Holocene summer cooling (Madsen and Thorsteinsson, 2001).

4.2.2. After 1850 AD

After 1850 a warming trend is imposed to simulate the post-LIA evolution of the ice cap. The magnitude of this post-LIA warming plays an important role as it determines how the pre-industrial temperature compares to the present-day temperature. An increase in air temperature over northern Greenland occurred since the end of the pre-industrial era (e.g. Kobashi et al., 2013), but the exact magnitude of the warming over the Hans Tausen Iskappe is unknown. By compiling information from several meteorological stations and applying a linear regression, Box (2013) found a Greenland average warming of +1.8 °C (+1.1 °C for summer) for the period 1840–2010. A substantial part of this warming occurs after 1990. When the mid 19th century is compared to the second part of the 20th century the annual temperature increase is typically somewhere between +0.5° and +1.0 °C. Based on Twentieth Century Reanalysis (20CR) and European Centre for Medium-Range Weather Forecasts (ECMWF) meteorological reanalyses for the period 1870–2010, Hanna et al. (2011) find similar average Greenland warming trends. The warming over Hans Tausen Iskappe was, however, more pronounced than the Greenland average (Hanna et al., 2011). To account for this range we consider three different temperature forcings, which respectively correspond to a +1.0 °C, +1.5 °C and +2.0 °C warming between 1850 (approx. end of the pre-industrial period) and the period 1961–1990 (see Fig. 3b). For these three temperature forcings the late 20th century and early 21st century temperatures are unprecedented in the past millennia. This recent unprecedented warm period is in line with (i) palaeorecords for other locations in northern Greenland and Arctic Canada (Kaufman et al., 2009; Fisher et al., 2012; Lecavalier et al., 2017), (ii) a record from a nearby lake (Perren et al., 2012) and (iii) information from the local ice core drilled at the Central Dome, which suggests that present-day temperature (after 1990) were warmer than anything recorded during the ice core record (last 3.5–4.0 ka) (Reeh, 1995; Clausen et al., 2001). A lower post-LIA year-round temperature increase (<1 °C) would be in contrast to this unprecedented millennial warm period, while a temperature forcing with a more pronounced warming trend (>2 °C) is not in line with the instrumental records.

4.3. Precipitation forcing

It is not possible to directly deduce past accumulation rates from

the Central Dome ice core due to the presence of many melt layers and the lack of fabric (distribution of crystallographic orientations) analyses (Clausen et al., 2001). However a qualitative interpretation of the ice core suggests that over its lifespan (the past 3.5–4.0 ka) the precipitation may for certain periods have been up to twice as high compared to present (Madsen and Thorsteinsson, 2001). This is particularly the case in the older parts of the record, at the time of build-up (Madsen and Thorsteinsson, 2001). The potential substantially higher precipitation is linked to periods with absence of permanent sea-ice, due to which the surrounding ocean could act as a moisture source (Reeh et al., 1999; Reeh, 2004; Funder et al., 2011a; Bintanja and Selten, 2014; Vihma, 2014). The absence/presence of sea-ice cannot directly be related to air temperature, as also water temperature and potential seasonal ice drift play an important role. This is for instance clear from the fact that today's air temperatures are the highest in the last millennia, but despite this the semi-permanent sea-ice is still present, which was not the case around 3–2.5 ka BP, when air temperatures were lower.

Here we impose a change in precipitation regime at 2.5 ka BP. After 2.5 ka BP the 1961–1990 precipitation field is scaled based on a Clausius-Clapeyron relationship set to 8% $°C^{-1}$ (Bintanja and Selten, 2014). Before 2.5 ka BP the Clausius-Clapeyron relationship is also used to scale the present-day precipitation field, but on top of this an additional precipitation forcing is applied, of +0% (*neutral*), +30% (*wet*) or +60% (*very wet*) (Fig. 4). This strong and sudden transition in precipitation regime is based on several local palaeorecords that indicate that year-round sea ice appeared around that time for high latitude coasts of Greenland and eastern Arctic Canada (e.g. Fisher et al., 2006; Polyak et al., 2010; Olsen et al., 2012). The most compelling evidence comes from dated driftwood fragments, which were precluded from penetrating the fjords after the landfast sea-ice became permanent. In a larger scale study Funder et al. (2011a) dated nearly 100 driftwood samples from Greenland coasts north of 80°N and found a strong drop around 3.0–2.5 ka BP. This is also the case for the immediate surroundings of Hans Tausen Iskappe, where the driftwood fragments strongly drop after 2.5 ka BP (Bennike, 1987; Landvik et al., 2001). Another indication of a change in sea-ice conditions around 2.5 ka BP may be the disappearance of Inuit settlements in northern Greenland, at the end of the Independence II culture, around 2400 cal BP (Andreasen, 1996; Landvik et al., 2001; Grønnow and Jensen, 2003). Potentially this migration may be related to a precipitation decrease, which strongly impacted the local vegetation (e.g. Gajewski, 2015).

4.4. Bedrock elevation changes

GIA had a significant impact on the Holocene evolution of the GrIS and its surrounding GICs (Wake et al., 2016). Over the Hans Tausen domain the Holocene GIA signal was dominated by a bedrock uplift motion as a response to an ice unloading over the GrIS. The magnitude of this local uplift (Fig. 5) is obtained from a coupled GrIS glaciological – GIA model, hereafter referred to as 'revised HUY3' (Lecavalier et al., 2017), which is constrained with local bedrock and sea-level change proxies. This change in bedrock elevation is applied uniformly over the whole ice cap domain. The effect of the local ice unloading over Hans Tausen was also investigated and found to be less than 0.5 m over the Holocene time period and is therefore negligible compared to the large-scale effect originating from a deglaciating GrIS.

The rise of the bedrock is particularly pronounced for the early Holocene: e.g. between 10.5 and 6.0 ka BP the bedrock elevation increased by 120 m (27 mm a^{-1} on average), while after this period the bedrock only rose by 37 m (6 mm a^{-1} on average). Given the July temperature lapse rate of −5.6 °C/km used in this study (Zekollari et al., 2017), temperatures over Hans Tausen Iskappe decreased by 0.9 °C over the last 10.5 ka due to bedrock uplift.

5. Modelled Holocene evolution

5.1. Fulfilling the constraints

The three main constraints on the ice cap evolution are (i) a mid Holocene disappearance of ice at the location of the present-day Central Dome, (ii) a reoccurrence of ice at the Central Dome around 4 ka BP, and (iii) the evolution towards the present-day ice cap.

5.1.1. Standard run (temperature forcing b)

For the intermediate temperature forcing (*b*) (see Fig. 3b) the three constraints are fulfilled when starting at or before 8.5 ka BP and by applying the *wet* precipitation forcing (bold lines in Fig. 6). Under the same temperature forcing (*b*) and considering another precipitation regime, the constrained ice cap cannot be reproduced. For a lower precipitation regime (*neutral* precipitation forcing), the

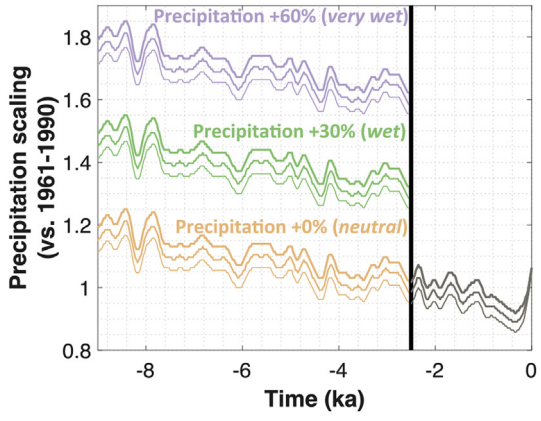

Fig. 4. Different precipitation forcing histories. The black vertical line delineates the transition from a high precipitation regime (before 2.5 ka BP) to the present-day precipitation regime (grey lines). Each cluster of precipitation histories consists of three lines, of which the highest line corresponds to the temperature forcing *a*, the middle line to the temperature forcing *b* and the lowest line to the temperature forcing *c* (see Fig. 3).

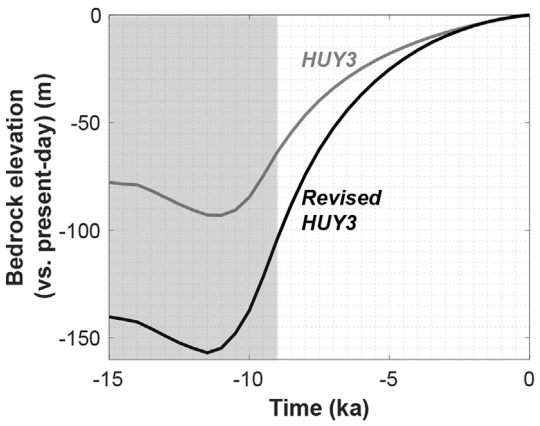

Fig. 5. Bedrock elevation change over Hans Tausen Iskappe since 15 ka BP. The shaded area corresponds to the period prior to the model simulations, the white area is the period over which the simulations are performed. The black line is the reconstruction used in this study, '*revised HUY3*' (Lecavalier et al., 2017), while the grey line is the older '*HUY3*' reconstruction (Lecavalier et al., 2014).

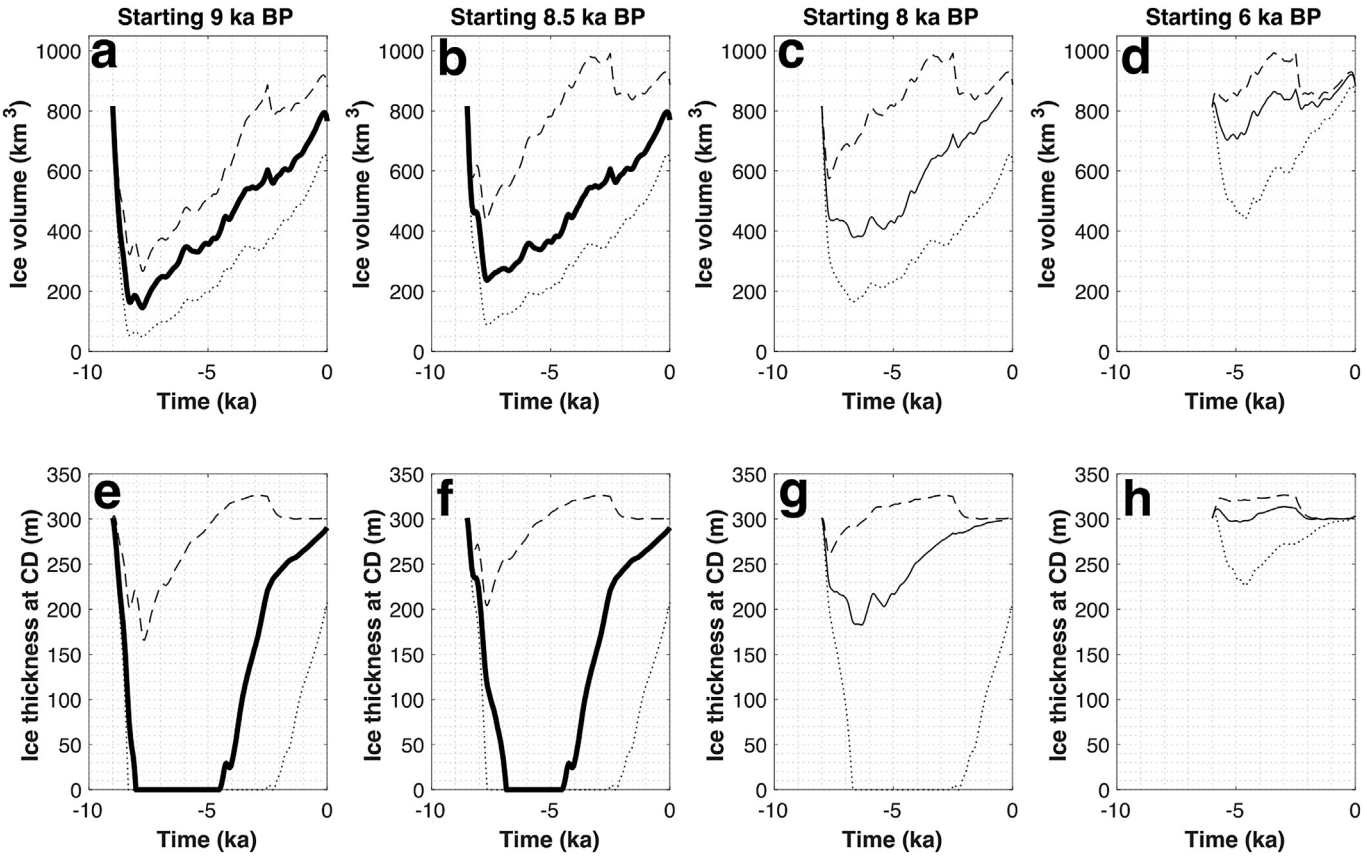

Fig. 6. Evolution of ice volume (a–d) and ice thickness at Central Dome (e–h) for temperature forcing *b*, with different starting periods. In each panel the upper, middle and lower line corresponds respectively to a *very wet* (+60%), *wet* (+30%) and *neutral* (+0%) precipitation forcing before 2.5 ka BP (see Fig. 4). The thick lines in a,b,e,f correspond to the forcings that produce a realistic present-day geometry and a timing of appearance for the ice at Central Dome in accordance with the ice core record.

ice at Central Dome only reappears around 2 ka BP (Fig. 6e and f) and the present-day ice cap is too small (Fig. 6a and b). On the other hand, under a higher precipitation regime (*very wet*) the Holocene ice thickness at Central Dome never drops below 165 m (Fig. 6e and f) and the modelled present-day ice cap is too large (Fig. 6a and b).

The starting time of the experiment also has a large impact on the long-term Holocene evolution of Hans Tausen Iskappe, as the constrained evolution cannot be reproduced for experiments starting at 8 ka BP or later. When starting at 8 ka BP, the ice at the location of the Central Dome does not disappear (Fig. 6g), except under *neutral* precipitation forcing, but in that case the ice here reappears only at 2.5 ka BP and the modelled present-day ice cap is too small (Fig. 6c). For an even later start, e.g. at 6 ka BP, the ice thickness at Central Dome hardly changes over time (Fig. 6h) and the obtained present-day ice cap is too large (Fig. 6d).

The simulation fulfilling the ice cap evolution constraints (temperature forcing *b* - *wet* precipitation) was also performed at a lower resolution (500 m) and using the Shallow-Ice Approximation (SIA), in which only local stresses are accounted for (Hutter, 1983). At a 500-m spatial resolution the ice cap evolution is almost unaltered compared to the original 250-m model simulation (Fig. 7.). When calculating the ice flow from the SIA, the areal evolution of the ice cap is almost identical compared to the original higher-order solution (Fig. 7 b). The volume evolution is also very similar (Fig. 7 a), although the volume is slightly higher for the HO solution (ca. 3–5%).

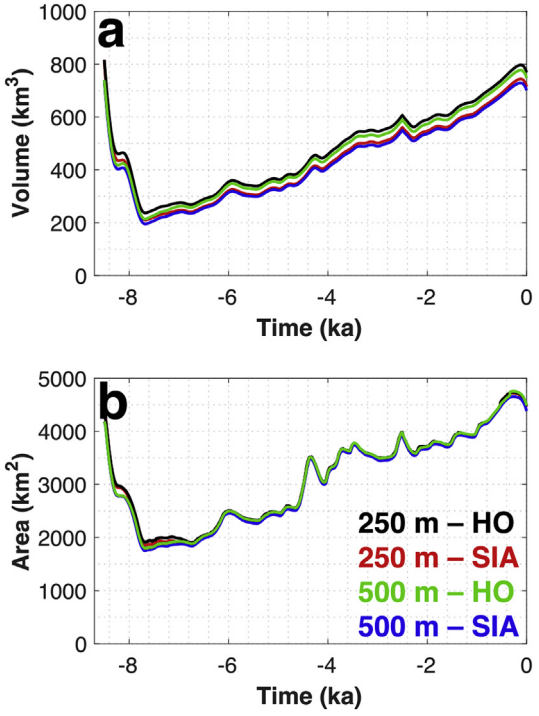

Fig. 7. Evolution of volume and area for different model complexity and model resolution. All simulations are run with temperature forcing *b*, *wet* precipitation, starting at 8.5 ka BP.

5.1.2. Alternative temperature forcing (a and c)

Under a warmer (temperature forcing *a*) or colder (temperature

forcing *c*) Holocene temperature evolution, the main findings are the same as for the intermediate temperature forcing (*b*). The Holocene evolution of the ice cap can be reconstructed fulfilling the three main constraints (i.e. Central Dome ice cover history and present-day state) when starting at or before 8.5 ka BP from a present-day steady state (Fig. 8). For the warmer temperature forcing (*a*) the *very wet* precipitation forcing is needed, while for the colder temperature forcing (*c*), no additional precipitation (*neutral* forcing) is required to reproduce the Holocene evolution of the ice cap.

5.2. Geometry evolution

For simulations fulfilling the three constraints on the ice cap evolution, the behaviour over the northern and the southern plateau is strongly distinct. The northern plateau remains largely ice covered during the entire Holocene and a local minimum in ice extent is reached at 7.5 ka BP (Fig. 9b). After this the northern part of the ice cap expands and thereafter remains generally stable, except for some fluctuations of the outlet glaciers. The southern part of the ice cap on the other hand largely disappears during the HTM and is mostly ice-free between 6.5 and 4.5 ka BP (see Fig. 9).

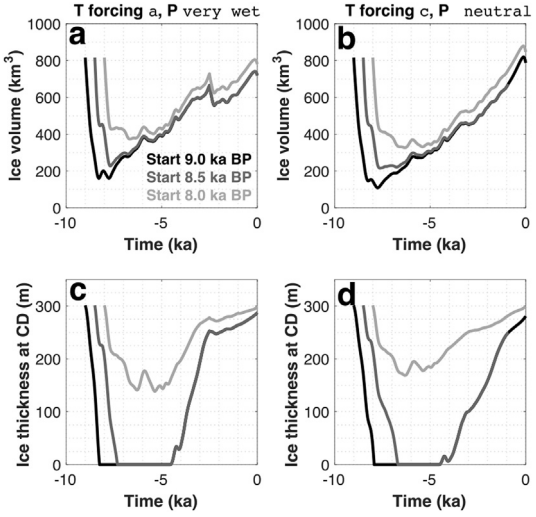

Fig. 8. Evolution of volume and ice thickness at Central Dome for temperature forcing *a* and *c*. In each plot 3 simulations are considered: starting at 9.0 ka, 8.5 ka BP and 8.0 ka BP.

The main driver for the contrasting behaviour between the northern and southern part of the ice cap is the SMB-elevation feedback. This is illustrated by the time lag between the total ice cap volume evolution and the ice thickness evolution at the Central Dome (Fig. 6b,f). After reaching a minimum at 8.0–7.5 ka BP the total ice cap volume starts to expand as a response to climatic cooling and a bedrock uplift. This mass gain is driven by an expanding ice mass on the northern plateau (see Fig. 9b and c). At the same time (7.5–6.5 ka BP), the southern part of the ice cap is still losing mass as locally the decrease in surface elevation has a stronger (negative) effect on the SMB than the positive contribution from the climatic cooling and GIA. This trend persists and eventually all ice is lost on the southern plateau around 6.5 ka BP. For about 2 ka the southern plateau remains largely ice free, after which a quick build-up of the ice cap occurs (Fig. 6e and f), driven by a mass supply originating from the northern part of the ice cap (see Fig. 9c,d,e) and reinforced through the SMB-elevation feedback.

6. Discussion

6.1. Palaeoglaciological and climatic implications

6.1.1. Deglaciation, HTM state and subsequent regrowth

In order to reproduce the collapse of the southern part of the ice cap and the disappearance of ice at the Central Dome, and taking into account the local palaeorecords, our results indicate that the ice cap must have had roughly its present-day extent sometime between 9.0 and 8.5 ka BP. This is believed to be in relatively good agreement to the reconstructed evolution of Flade Isblink (80.5–82°N, ca. 8000 km^2, about 300 km to the east) around this period. This ice cap was also part of the GrIS during the previous

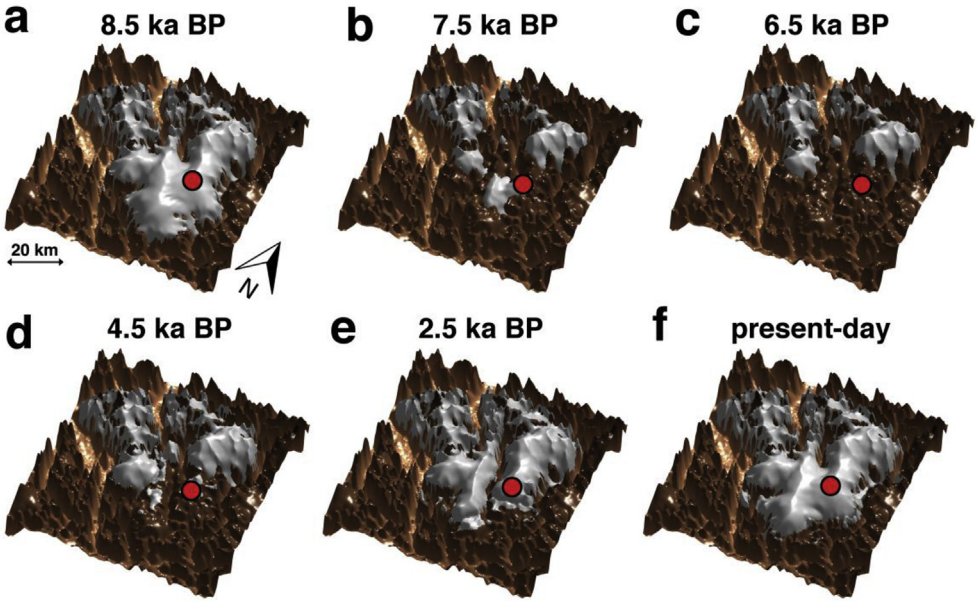

Fig. 9. Evolution of the ice cap geometry for temperature forcing *b*, with the *wet* precipitation forcing, starting at 8.5ka BP (Fig. 5b,f). The red dots indicates the location of the present-day Central Dome. (For interpretation of the references to colour in this figure legend, the reader is referred to the web version of this article.)

glacial period and roughly had its present-day size around 9–8 ka BP (Hjort, 1997). Also for later periods Flade Isblink may have evolved in a similar way as the modelled evolution of Hans Tausen Iskappe, with a strong regrowth starting at 5–4 ka BP and a LIA maximum Neoglacial extent (Hjort, 1997). This is in contrast with Renland Iskappe located in Scoresby Sund (71°N, eastern Greenland). An ice core drilled to the bed of Renland Iskappe (Johnsen et al., 2001) indicates that the ice cap was far more stable than Hans Tausen Iskappe during the Holocene. This is confirmed by first results from the 2015 RECAP (REnland ice CAp Project) ice core drilling (Vinther, 2016; Kjær et al., 2017; Maffezzoli et al., 2017), which suggest that ice from the entire previous glacial period is preserved. The stability of the Renland Iskappe may in part be related to the different climatic conditions, but it is likely also caused by a different topographic setting. At present most of Renland Iskappe is situated above 1500 m with local domes above 2300 m a.s.l. (Johnsen et al., 1992), which is well above the equilibrium line altitude, and makes the ice cap less susceptible to a warmer climate. The importance of the topographic setting is also illustrated by the neighbouring Bregne Iskappe, for which the evolution is again more similar to the one of Hans Tausen Iskappe and Flade Isblink Iskappe. Bregne Iskappe was close to its present-day position around 10.7 ka BP, then completely disappeared and subsequently reappeared in the last 2–3 millennia (Levy et al., 2014).

Whereas the disappearance of the southern part of the ice cap is derived from the Central Dome ice core, the Holocene evolution for the northern part of the ice cap is far more debated. Reeh (1995) and Thomsen et al. (1996) analysed oxygen isotopes from outlet glaciers in the northern part of the ice cap and interpreted the lack of any glacial ice as an indication for a complete disappearance of the ice cap during the HTM. However, in all model runs performed here, forced with climatic reconstructions in accordance with palaeorecords, the northern part of the ice cap is continuously and largely ice covered during the entire Holocene. Even under temperature forcing *a*/*neutral* precipitation, which corresponds to the most negative SMB conditions possible in our setup (which is far too low to reproduce a regrowth of the southern ice cap and which produces a too small present-day ice cap), a part of the ice cap on the northern plateau still survives the HTM.

Experiments starting from an ice-free surface at 6 ka BP and 4 ka BP indicate that the present-day ice cap can be entirely build up in a few millennia (see Fig. 10). These time scales for build-up suggest that a present-day ice cap with only Holocene ice is possible, but also indicate that the ice transfer from the accumulation area to the ablation area must occur fast. It is thus not surprising that only Holocene ice was found in the outlet glaciers. This is also supported by a 500–1000 year old musk-ox that melted out close to the snout of Hare outlet glacier (NE) (see Fig. 1), where the oldest ice is expected (Thomsen et al., 1996). We therefore suggest that all ice did not disappear during the HTM and that the northern part of the ice cap was never completely ice-free.

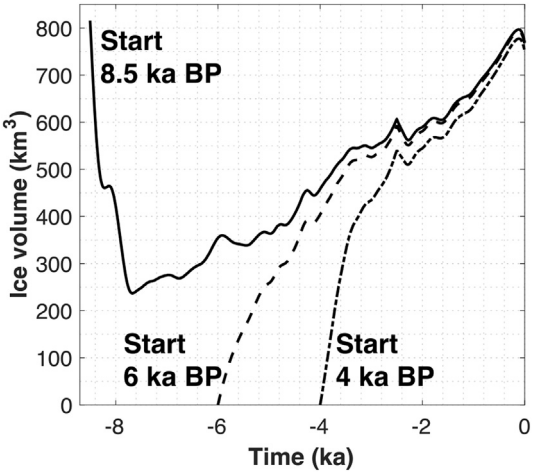

Fig. 10. Evolution of ice volume for different initial conditions: starting from the steady state ice cap (at 8.5 ka BP) or an ice-free surface (at 6 and 4 ka BP). All simulations are run with temperature forcing *b* and *wet* precipitation.

6.1.2. Role of increased precipitation

The ice cap evolution under various temperature forcings can be reproduced with different precipitation regimes. For the warmest Holocene temperature forcing (*a*), the precipitation until 2.5 ka BP must have been typically around 65–85% higher than at present (*very wet* precipitation) to accurately reproduce the ice cap evolution (see Fig. 4). Under slightly colder conditions (temperature forcing *b*) precipitation must have been around 30–50% higher than at present, while under the coldest forcing (*c*), no additional precipitation forcing is needed compared to present-day and the Holocene precipitation fluctuated 15% around the 1961–1990 level (through the Clausius-Clapeyron relationship, see Fig. 4). The model output thus suggests that the effect of the sea-ice absence on the precipitation may range from (almost) inexistent to substantial. The suggested doubled precipitation compared to the present-day around 4 ka BP based on a qualitative interpretation of the ice core (Madsen and Thorsteinsson, 2001), or even tripled precipitation during the HTM (Reeh et al. (2001), is thus not supported by the modelling evidence presented here). In the most wet case under which the constraints on the ice cap evolution are fulfilled (temperature forcing *a*, *very wet*) the precipitation at 4 ka BP is only about 70% higher than at present.

6.1.3. Role of isostatic uplift

The Holocene bedrock uplift over the Hans Tausen domain (Fig. 5) positively contributes to the SMB as it lowers the surface temperature. Although the magnitude of the cooling induced by the bedrock uplift is only on the order of 1 °C over the Holocene (see section 4.4.), its timing is important for the ice cap Holocene evolution. Under a previous GrIS deglaciation reconstruction, using the '*HUY3*' model (Lecavalier et al., 2014; Sinclair et al., 2016), for which the temperature forcing was not corrected for the effect of a changing IIS, the Holocene GIA over Hans Tausen is less pronounced (see Fig. 5). The bedrock elevation during the Early Holocene is therefore relatively higher compared to the '*revised HUY3*' reconstruction used in this study (Lecavalier et al., 2017), leading to a more positive SMB. As a consequence less ice is lost at the HTM (Fig. 11a) and the disappearance of ice at the Central Dome cannot be reproduced under any realistic climatic forcing (Fig. 11b). The importance of the Holocene bedrock evolution on the modelled evolution is particularly clear for a simulation where the bedrock elevation is kept constant at the present-day level throughout the Holocene. Under these conditions the SMB is in all cases too positive. As a consequence the ice thickness at the Central Dome hardly changes over time and the partial disappearance of the ice cap and subsequent regrowth to its present-day geometry cannot be reproduced.

6.2. Little Ice Age, present-day state and implications for future ice cap evolution

The modelled LIA volume and extent of the ice cap are the largest since the HTM. In the present-day landscape many moraine ridges from the LIA are visible in the vicinity of present-day glacier

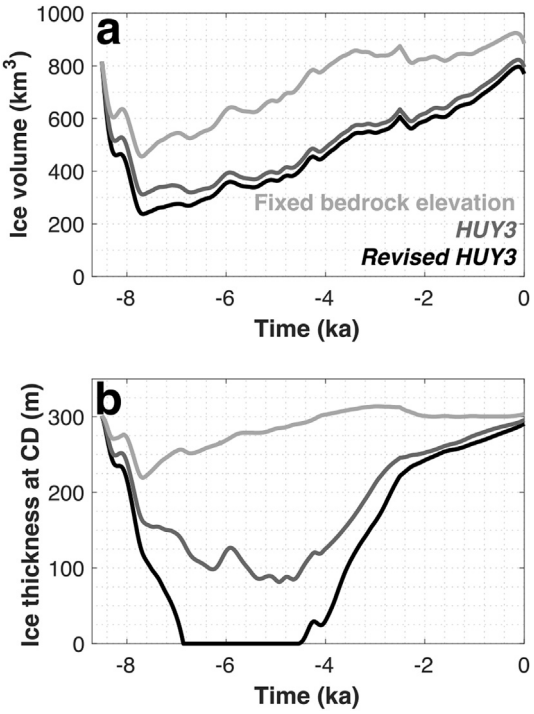

Fig. 11. Evolution of ice volume and ice thickness at Central Dome under different GIA forcings. For all simulations the temperature forcing *b* is used with the *wet* precipitation forcing, starting at 8.5 ka BP. The black line corresponds to the standard run (forced with '*revised HUY3*', Lecavalier et al. (2017)), while the dark grey line corresponds to a run forced with 'HUY3' (Lecavalier et al., 2014). In the 'Fixed bedrock elevation' experiment (light grey line) the bedrock elevation does not change over time, i.e. the present-day elevation is maintained throughout the entire Holocene.

snouts, which contrasts with the old landscape in which pronounced moraine ridges are absent (Landvik et al., 2001). These are the only moraines from after the HTM and therefore suggest that the LIA geometry had the largest extent since then. After the LIA the ice cap slightly retreated to its present-day position, typically by several hundred meters to a few kilometres, which is of the same order as our modelled retreat under a 1–2 °C warming between 1850 and 1961–1990. The impact of the post-LIA warming on the long-term evolution of the ice cap is evident from the ice volume evolution (Figs. 6, 7, 10 and 11), where a slight decline is observed on a long-term growth trend. The fact that the late 20th century ice cap changes only little under 1961–1990 climatic conditions, which produce a near-zero SMB (Zekollari et al., 2017), is therefore related to a balancing of the long-term growth trend and short-term retreat trend, rather than being an indication that the present-day ice cap is in steady state.

At present the ice cap is still surrounded by semi-permanent sea ice (Polyak et al., 2010; Funder et al., 2011a), but in a warming climate it is projected that this sea-ice will disappear (Overland and Wang, 2013). Based on the Holocene simulations presented here, it is expected that the effect on the precipitation will be somewhere between very limited and an increase by up to 60%. The upper end of this range, is close to the 21st century precipitation increase predicted by CMIP5 climate models under the most extreme temperature forcing (RCP8.5), which is around 50–60% (2091–2100 vs. 2006–2015) (Bintanja and Selten, 2014). Based on a previous study on the sensitivity of the ice cap (Zekollari et al., 2017), we predict that such an increase will be far too limited to substantially counteract the mass loss related to a temperature increase. Furthermore, in a warming climate, rain is projected to become the dominant form of precipitation at high latitudes (>70%) at the expense of snow fall (Bintanja and Andry, 2017). The ice cap is therefore expected to entirely disappear after a period between 200 and 250 years (extreme temperature forcing, RCP8.5) and 400–500 years (intermediate warming, RCP4.5).

6.3. Effects of model complexity and resolution

The effect of model complexity and resolution on the evolution of ice masses is of large interest, as in many cases a trade-off has to be made between computational costs and improved model complexity and resolution (e.g. Le Meur et al., 2004; Leysinger Vieli and Gudmundsson, 2004; Fürst et al., 2013). The simulations performed here at a lower resolution (500 m) and/or using the SIA indicate that the differences with the standard run (250 m, HO) are very limited (Fig. 7.). The few small differences that occur in volume and area are mainly related to the small velocity differences occurring in the outlet glaciers (Zekollari et al., 2017).

From this we can conclude that for the long-term evolution of the ice cap the model complexity and resolution are of limited importance. This is in contrast with present-day study on the dynamics of Hans Tausen Iskappe (Zekollari et al., 2017), where the model resolution and complexity were found to have a relatively important effect. Despite the inaccuracies in the SIA (e.g. Jouvet, 2016) and the implications this has, also for palaeoglaciological studies (e.g. Kirchner et al., 2016), here the use of a computationally more demanding non-local ice flow solution has limited added value. This does not imply that the ice dynamics are unimportant, but suggest that changes in SMB are far more important drivers for the Holocene evolution of the ice cap. For the ice cap decay and build-up the ice flow from the northern plateau to the southern part of the ice cap was shown to be crucial (see 5.2.), and this large-scale component is also well captured under the SIA and at lower spatial resolution.

7. Conclusions

In this study, we simulated for the first time the full transient Holocene evolution of a high Arctic ice cap with a 3-D higher-order thermo-mechanical ice flow – SMB model. The obtained results (i) allow us to better constrain the Holocene evolution of the world's northernmost ice cap, (ii) improve our understanding of the evolution of the palaeoclimate of the high Arctic, and (iii) have several implications for palaeomodelling studies on individual ice caps.

(i) The simulations suggest that in order to reproduce the HTM disappearance of ice at the Central Dome, Hans Tausen Iskappe had an extent and geometry that was roughly similar to the present-day one sometime between 9.0 and 8.5 ka BP. The debated entire disappearance of the ice cap during the HTM is not reproduced and it is argued that most of the northern plateau remained ice covered throughout the Holocene. Due to the SMB-elevation feedback the evolution of the northern and southern part of the ice cap is asynchronous, and whereas the northern part of the ice cap reached its minimum around 7.5 ka BP, the southern part of the ice cap becomes only ice-free at 6.5 ka BP. A build-up of the southern ice cap started around 4 ka BP and continued until the end of the LIA, after which a marked retreat occurred to its present-day position. The earlier finding that the present-day ice cap hardly changes under the 1961–1990 climatic conditions (Zekollari et al., 2017) does therefore not imply a late 20th century steady state ice cap, but rather suggests it is influenced by a counterbalancing long-term Holocene growth and a short-term post-LIA retreat.

(ii) The Holocene evolution of the ice cap was reproduced with a pre-industrial temperature record derived from the Agassiz ice cap. The fact that the ice cap evolution could be reproduced relatively well, fulfilling all constraints, supports the hypothesis that the changes in the Holocene climate were relatively similar over northern Greenland and eastern Arctic Canada. The other high latitude large ice cap in Greenland, Flade Isblink, is believed to have evolved in a somewhat similar way as Hans Tausen Iskappe. Linking the Agassiz pre-industrial temperature record to a post-LIA warming trend to force the model suggests that the warming between 1850 and the period 1961–1990 was between 1.0 °C and 2.0 °C over Peary Land. Based on the model simulations it is not possible to make strict quantitative statements about past precipitation, but it is unlikely that precipitation was, as suggested earlier, twice or three times as high as at present around 4.0–3.5 ka BP. In the most extreme case (assuming a relatively warm Holocene) the precipitation may have been up to 70% higher about 4 ka BP. This finding, combined with a previous study on the sensitivity of the ice cap to climatic changes, suggests that the future increase in precipitation due to a loss of the semi-permanent sea ice will be insufficient to substantially counteract the ice loss in a warming climate.

(iii) The long-term ice cap evolution is mainly driven by SMB changes. The ice flow needs to be taken into account to simulate the supply from the northern to the southern part plateau, which is crucial during the Holocene ice cap build-up. We show that a simple SIA model run at a relatively low resolution (500 m) is sufficient to reproduce this mass transfer. The inclusion of longitudinal stresses (HO solution) and a higher spatial resolution (250 m) were found to be of limited added value, as their effect is smaller than uncertainties related to the model setup. On the other hand the bedrock uplift (GIA) over Hans Tausen had to be accounted for as without this the constraints on the Holocene ice cap evolution could not be reproduced. Our results therefore suggest that modelling studies of millennial-scale ice cap evolution should focus on SMB and boundary conditions, such as the climate forcing and GIA, rather than on complex ice dynamics.

Acknowledgments

We thank A.P. Ahlstrøm, C. Hvidberg, H. Machguth and A.M. Solgaard for their help in retrieving documentation from the Hans Tausen expeditions in the 1990s. The manuscript greatly benefited from comments by Nicolaj K. Larsen and an anonymous reviewer. H. Zekollari holds a PhD fellowship of the Research Foundation – Flanders (FWO-Vlaanderen).

References

Andreasen, C., 1996. A survey of paleo-Eskimo sites in northern Eastgreenland. In: The Paleo-Eskimo Cultures of Greenland. New Perspectives in Greenlandic Archaeology. Danish Polar Center, Copenhagen, pp. 177–189.

Balascio, N.L., D'Andrea, W.J., Bradley, R.S., 2015. Glacier response to North Atlantic climate variability during the Holocene. Clim. Past. 11, 1587–1598. http://dx.doi.org/10.5194/cp-11-1587-2015.

Bennike, O., 1987. Quaternary geology and biology of the Jörgen Brönlund Fjord area, North Greenland. Meddelelser Om. Grønl. Geosci. 18, 23.

Bennike, O., Björck, S., 2002. Chronology of the last recession of the Greenland ice sheet. J. Quat. Sci. 17, 211–219. http://dx.doi.org/10.1002/jqs.670.

Bennike, O., Weidick, A., 1999. Observations on the quaternary geology around Nioghalvfjerdsfjorden, eastern North Greenland. Geol. Greenl. Surv. Bull. 183, 57–60.

Berger, A., Loutre, M.F., 1991. Insolation values for the climate of the last 10 million years. Quat. Sci. Rev. 10, 297–317. http://dx.doi.org/10.1016/0277-3791(91)90033-Q.

Bintanja, R., Andry, O., 2017. Towards a rain-dominated Arctic. Nat. Clim. Chang. http://dx.doi.org/10.1038/nclimate3240.

Bintanja, R., Selten, F.M., 2014. Future increases in Arctic precipitation linked to local evaporation and sea-ice retreat. Nature 509, 479–482. http://dx.doi.org/10.1038/nature13259.

Box, J.E., 2013. Greenland ice sheet mass balance reconstruction. Part II: surface mass balance (1840-2010). J. Clim. 26, 6974–6989. http://dx.doi.org/10.1175/JCLI-D-12-00518.1.

Briner, J.P., McKay, N.P., Axford, Y., Bennike, O., Bradley, R.S., de Vernal, A., Fisher, D., Francus, P., Fréchette, B., Gajewski, K., Jennings, A., Kaufman, D.S., Miller, G., Rouston, C., Wagner, B., 2016. Holocene climate change in Arctic Canada and Greenland. Quat. Sci. Rev. 147, 340–364. http://dx.doi.org/10.1016/j.quascirev.2016.02.010.

Clausen, H.B., Stampe, M., Hammer, C.U., Hvidberg, C.S., Dahl-Jensen, D., Steffensen, J.P., 2001. Glaciological and chemical studies on ice cores from Hans Tausen ice cap, Greenland. Meddelelser Om. Grønl. Geosci. 39, 123–149.

Collins, M., Knutti, R., Arblaster, J., Dufresne, J.-L., Fichefet, T., Friedlingstein, P., Gao, X., Gutowski, W.J., Johns, T., Krinner, G., Shongwe, M., Tebaldi, C., Weaver, A.J., Wehner, M., 2013. Long-term climate change: projections, commitments and irreversibility. In: Stocker, T.F., Qin, D., Plattner, G.K., Tignor, M., Allen, S.K., Boschung, J., Nauels, A., Xia, Y., Bex, V., Midgley, P.M. (Eds.), Climate Change 2013: the Physical Science Basis. Contribution of Working Group I to the Fifth Assessment Report of the Intergovernmental Panel on Climate Change. Cambridge University Press, Cambridge, U.K., pp. 1029–1136. http://dx.doi.org/10.1017/CBO9781107415324.024

Davies, W., Krinsley, D., 1962. The recent regimen of the ice cap margin in North Greenland. Int. Assoc. Sci. Hydrol. 58 (58), 119–130.

Fisher, D., Dyke, A., Koerner, R., Bourgeois, J., Kinnard, C., Zdanowicz, C., de Vernal, A., Hillaire-Marcel, C., Savelle, J., Rochon, A., 2006. Natural variability of Arctic sea ice over the Holocene. Eos, Trans. Am. Geophys. Union. http://dx.doi.org/10.1029/2006EO280001.

Fisher, D., Koerner, R., 2003. Holocene ice-core climate history, a multi-variable approach. In: Mackay, A., Battarbee, R., Birks, J., Oldfield, F. (Eds.), Global Change in the Holocene. Arnold, London, pp. 281–293.

Fisher, D., Zheng, J., Burgess, D., Zdanowicz, C., Kinnard, C., Sharp, M., Bourgeois, J., 2012. Recent melt rates of Canadian arctic ice caps are the highest in four millennia. Glob. Planet. Change 84–85, 3–7. http://dx.doi.org/10.1016/j.gloplacha.2011.06.005.

Flowers, G.E., Björnsson, H., Geirsdóttir, Á., Miller, G.H., Black, J.L., Clarke, G.K.C., 2008. Holocene climate conditions and glacier variation in central Iceland from physical modelling and empirical evidence. Quat. Sci. Rev. 27, 797–813. http://dx.doi.org/10.1016/j.quascirev.2007.12.004.

Funder, S., Abrahamsen, N., 1988. Palynology in a polar desert, eastern North Greenland. Boreas 17, 195–207.

Funder, S., Goosse, H., Jepsen, H., Kaas, E., Kjær, K.H., Korsgaard, N.J., Larsen, N.K., Linderson, H., Lyså, A., Möller, P., Olsen, J., Willerslev, E., 2011a. A 10,000-year record of Arctic Ocean sea-ice variability - view from the Beach. Science 333, 747–750. http://dx.doi.org/10.1126/science.1202760.

Funder, S., Jennings, A., Kelly, M., 2004. Middle and late quaternary glacial limits in Greenland. In: Ehlers, J., Gibbard, P. (Eds.), Developments in Quaternary Science. Elsevier, Amsterdam, pp. 425–430. http://dx.doi.org/10.1016/S1571-0866(04)80210-0.

Funder, S., Kjeldsen, K.K., Kjær, K.H., O Cofaigh, C., 2011b. The Greenland ice sheet during the past 300,000 Years. A Rev. Dev. Quat. Sci. 15, 699–713. http://dx.doi.org/10.1016/B978-0-444-53447-7.00050-7.

Fürst, J.J., Goelzer, H., Huybrechts, P., 2013. Effect of higher-order stress gradients on the centennial mass evolution of the Greenland ice sheet. Cryosph 7, 183–199. http://dx.doi.org/10.5194/tc-7-183-2013.

Fürst, J.J., Rybak, O., Goelzer, H., De Smedt, B., De Groen, P., Huybrechts, P., 2011. Improved convergence and stability properties in a three-dimensional higher-order ice sheet model. Geosci. Model Dev. 4, 1133–1149. http://dx.doi.org/10.5194/gmd-4-1133-2011.

Gajewski, K., 2015. Impact of Holocene climate variability on Arctic vegetation. Glob. Planet. Change 133, 272–287. http://dx.doi.org/10.1016/j.gloplacha.2015.09.006.

Gilbert, A., Glowers, G.E., Miller, G.H., Rabus, B.T., Van Wychen, W., Gardner, A.S., Copland, L., 2016. Sensitivity of Barnes Ice Cap, Baffin Island, Canada, to climate state and internal dynamics. J. Geophys. Res. Earth Surf. 121, 1516–1539. http://dx.doi.org/10.1002/2014JF003839.

Glen, J.W., 1955. The creep of polycrystalline ice. Proc. R. Soc. A Math. Phys. Eng. Sci. 228, 519–538. http://dx.doi.org/10.1098/rspa.1955.0066.

Goelzer, H., Huybrechts, P., Loutre, M.-F., Fichefet, T., 2016. Last Interglacial climate and sea-level evolution from a coupled ice sheet-climate model. Clim. Past. 12, 2195–2213. http://dx.doi.org/10.5194/cp-12-2195-2016.

Grønnow, B., Jensen, J.F., 2003. The northernmost ruins of the globe, in: Eigil Knuth's Archaeological investigations in Peary Land and adjacent areas of High Arctic Greenland. Medd. Gronl Man. Soc. 1–403.

Hammer, C.U., 2001. The Hans Tausen Ice Cap. Danish Polar Center, Copenhagen.

Hammer, C.U., Johnsen, S.J., Clausen, H.B., Dahl-Jensen, D., Gundestrup, N., Steffensen, J.P., 2001. The paleoclimatic record from a 345 m long ice core from the Hans Tausen Iskappe. Meddelelser Om. Grønl. Geosci. 39, 87–95.

Hanna, E., Huybrechts, P., Cappelen, J., Steffen, K., Bales, R.C., Burgess, E., McConnell, J.R., Steffensen, J.P., Van Den Broeke, M., Wake, L., Bigg, G., Griffiths, M., Savas, D., 2011. Greenland Ice Sheet surface mass balance 1870 to 2010 based on Twentieth Century Reanalysis, and links with global climate

forcing. J. Geophys. Res. Atmos. 116. http://dx.doi.org/10.1029/2011JD016387.
Hjort, C., 1997. Glaciation, climate history, changing marine levels and the evolution of the Northeast Water Polynya. J. Mar. Syst. 10, 23–33. http://dx.doi.org/10.1016/S0924-7963(96)00068-1.
Hutter, K., 1983. Theoretical Glaciology. Reidel Publ. Co., Dordrecht.
Huybrechts, P., 2002. Sea-level changes at the LGM from ice-dynamic reconstructions of the Greenland and Antarctic ice sheets during the glacial cycles. Quat. Sci. Rev. 21, 203–231. http://dx.doi.org/10.1016/S0277-3791(01)00082-8.
Huybrechts, P., 1996. Basal temperature conditions of the Greenland ice sheet during the glacial cycles. Ann. Glaciol. 23, 226–236.
Huybrechts, P., 1990. A 3-D model for the Antarctic ice sheet: a sensitivity study on the glacial-interglacial contrast. Clim. Dyn. 5, 79–92. http://dx.doi.org/10.1007/BF00207423.
Huybrechts, P., Goelzer, H., Janssens, I., Driesschaert, E., Fichefet, T., Goosse, H., Loutre, M.F., 2011. Response of the Greenland and Antarctic ice sheets to multi-millennial greenhouse warming in the earth system model of intermediate complexity LOVECLIM. Surv. Geophys. 32, 397–416. http://dx.doi.org/10.1007/s10712-011-9131-5.
Hvidberg, C.S., Keller, K., Gundestrup, N., Jonsson, P., 2001. Ice-divide flow at Hans Tausen Iskappe, North Greenland, from surface movement data. J. Glaciol. 47, 78–84. http://dx.doi.org/10.3189/172756501781832485.
Ingólfsson, Ó., Frich, P., Funder, S., Humlum, O., 1990. Paleoclimatic implications of an early Holocene glacier advance on Disko Island, West Greenland. Boreas 19, 297–311. http://dx.doi.org/10.1111/j.1502-3885.1990.tb00133.x.
Jakobsson, M., Andreassen, K., Bjarnadóttir, L.R., Dove, D., Dowdeswell, J.A., England, J.H., Funder, S., Hogan, K., Ingólfsson, Ó., Jennings, A., Krog Larsen, N., Kirchner, N., Landvik, J.Y., Mayer, L., Mikkelsen, N., Möller, P., Niessen, F., Nilsson, J., O'Regan, M., Polyak, L., Nørgaard-Pedersen, N., Stein, R., 2014. Arctic Ocean glacial history. Quat. Sci. Rev. 92, 40–67. http://dx.doi.org/10.1016/j.quascirev.2013.07.033.
Janssens, I., Huybrechts, P., 2000. The treatment of meltwater retention in mass-balance parameterizations of the Greenland ice sheet. Ann. Glaciol. 31, 133–140. http://dx.doi.org/10.3189/172756400781819941.
Johnsen, S.J., Clausen, H.B., Dansgaard, W., Fuhrer, K., Gundestrup, N., Hammer, C.U., Iversen, P., Jouzel, J., Stauffer, B., Steffensen, J.P., 1992. Irregular glacial interstadials recorded in a new Greenland ice core. Nature. http://dx.doi.org/10.1038/359311a0.
Johnsen, S.J., Dahl-Jensen, D., Gundestrup, N., Steffensen, J.P., Clausen, H.B., Miller, H., Masson-Delmotte, V., Sveinbjörnsdottir, A.E., White, J., 2001. Oxygen isotope and palaeotemperature records from six Greenland ice-core stations: camp Century, Dye-3, GRIP, GISP2, Renland and NorthGRIP. J. Quat. Sci. 16, 299–307. http://dx.doi.org/10.1002/jqs.622.
Jouvet, G., 2016. Mechanical error estimators for shallow ice flow models. J. Fluid Mech. 807, 40–61. http://dx.doi.org/10.1017/jfm.2016.593.
Kaufman, D.S., Ager, T.A., Anderson, N.J., Anderson, P.M., Andrews, J.T., Bartlein, P.J., Brubaker, L.B., Coats, L.L., Cwynar, L.C., Duvall, M.L., Dyke, A.S., Edwards, M.E., Eisner, W.R., Gajewski, K., Geirsdóttir, A., Hu, F.S., Jennings, A.E., Kaplan, M.R., Kerwin, M.W., Lozhkin, A.V., MacDonald, G.M., Miller, G.H., Mock, C.J., Oswald, W.W., Otto-Bliesner, B.L., Porinchu, D.F., Rühland, K., Smol, J.P., Steig, E.J., Wolfe, B.B., 2004. Holocene thermal maximum in the western Arctic (0-180°W). Quat. Sci. Rev. 23, 529–560. http://dx.doi.org/10.1016/j.quascirev.2003.09.007.
Kaufman, D.S., Schneider, D.P., McKay, N.P., Ammann, C.M., Bradley, R.S., Briffa, K.R., Miller, G.H., Otto-Bliesner, B.L., Overpeck, J.T., Vinther, B.M., Arctic Lakes 2k Project Members, 2009. Recent Warming Reverses Long-Term Arctic Cooling. Science 325, 1236–1239. http://dx.doi.org/10.1126/science.1173983.
Kelly, M.A., Lowell, T.V., 2009. Fluctuations of local glaciers in Greenland during latest Pleistocene and Holocene time. Quat. Sci. Rev. 28, 2088–2106. http://dx.doi.org/10.1016/j.quascirev.2008.12.008.
Kirchner, N., Ahlkrona, J., Gowan, E.J., Lötstedt, P., Lea, J.M., Noormets, R., von Sydow, L., Dowdeswell, J.A., Benham, T., 2016. Shallow ice approximation, second order shallow ice approximation, and full Stokes models: a discussion of their roles in palaeo-ice sheet modelling and development. Quat. Sci. Rev. 135, 103–114. http://dx.doi.org/10.1016/j.quascirev.2016.01.013.
Kjær, H.A., Vallelonga, P., Vinther, B., Simonsen, M., Maffezzoli, N., Gkinis, V., Svensson, A., Jensen, C.M., Dallmayr, R., Spolaor, A., Edwards, R., 2017. Dansgaard-Oeschger cycles observed in the Greenland ReCAP ice core project. Geophys. Res. Abstr. 19. EGU2017–11565.
Kobashi, T., Shindell, D.T., Kodera, K., Box, J.E., Nakaegawa, T., Kawamura, K., 2013. On the origin of multidecadal to centennial Greenland temperature anomalies over the past 800 yr. Clim. Past. 9, 583–596. http://dx.doi.org/10.5194/cp-9-583-2013.
Landvik, J.Y., Weidick, A., Hansen, A., 2001. The glacial history of the Hans Tausen Iskappe and the last glaciation of Peary Land, North Greenland. Meddelelser Om. Grønl. Geosci. 39, 27–44.
Larsen, N.K., Funder, S., Linge, H., Möller, P., Schomacker, A., Fabel, D., Xu, S., Kjær, K.H., 2015. A Younger Dryas re-advance of local glaciers in north Greenland. Quat. Sci. Rev. http://dx.doi.org/10.1016/j.quascirev.2015.10.036.
Larsen, N.K., Kjær, K.H., Funder, S., Möller, P., van der Meer, J.J.M., Schomacker, A., Linge, H., Darby, D.A., 2010. Late Quaternary glaciation history of northernmost Greenland - evidence of shelf-based ice. Quat. Sci. Rev. 29, 3399–3414. http://dx.doi.org/10.1016/j.quascirev.2010.07.027.
Le Meur, E., Gagliardini, O., Zwinger, T., Ruokolainen, J., 2004. Glacier flow modelling: a comparison of the Shallow Ice Approximation and the full-Stokes solution. Comptes Rendus Phys. 5, 709–722. http://dx.doi.org/10.1016/j.crhy.2004.10.001.
Lecavalier, B.S., Fisher, D., Milne, G.A., Vinther, B., Tarasov, L., Huybrechts, P., Lacelle, D., Main, B., Zheng, J., Bourgeois, J., Dyke, A.S., 2017. A Holocene temperature record from the Agassiz ice cap: implications for high-Arctic climate change and Greenland ice sheet evolution. Proc. Natl. Acad. Sci. U. S. A. http://dx.doi.org/10.1073/pnas.1616287114. http://www.pnas.org/content/early/2017/05/15/1616287114.
Lecavalier, B.S., Milne, G.A., Simpson, M.J.R., Wake, L., Huybrechts, P., Tarasov, L., Kjeldsen, K.K., Funder, S., Long, A.J., Woodroffe, S., Dyke, A.S., Larsen, N.K., 2014. A model of Greenland ice sheet deglaciation constrained by observations of relative sea level and ice extent. Quat. Sci. Rev. 102, 54–84. http://dx.doi.org/10.1016/j.quascirev.2014.07.018.
Lecavalier, B.S., Milne, G.A., Vinther, B.M., Fisher, D.A., Dyke, A.S., Simpson, M.J.R., 2013. Revised estimates of Greenland ice sheet thinning histories based on ice-core records. Quat. Sci. Rev. 63, 73–82. http://dx.doi.org/10.1016/j.quascirev.2012.11.030.
Levy, L.B., Kelly, M.A., Lowell, T.V., Hall, B.L., Hempel, L.A., Honsaker, W.M., Lusas, A.R., Howley, J.A., Axford, Y.L., 2014. Holocene fluctuations of Bregne ice cap, Scoresby Sund, east Greenland: a proxy for climate along the Greenland Ice Sheet margin. Quat. Sci. Rev. 92, 357–368. http://dx.doi.org/10.1016/j.quascirev.2013.06.024.
Leysinger Vieli, G.J.-M.C., Gudmundsson, G.H., 2004. On estimating length fluctuations of glaciers caused by changes in climatic forcing. J. Geophys. Res. 109, F01007. http://dx.doi.org/10.1029/2003JF000027.
Madsen, K.N., Thorsteinsson, T., 2001. Textures, fabrics and meltlayer stratigraphy in the Hans Tausen ice core, North Greenland - indications of late Holocene ice cap generation? Meddelelser Om. Grønl. Geosci. 39, 97–114.
Maffezzoli, N., Vallelonga, P., Spolaor, A., Barbante, C., Edwards, R., Saiz-Lopez, A., Kjær, H.A., Simonsen, M., Vinther, B., 2017. 125,000 year Arctic sea ice variability from the Renland ice core. Geophys. Res. Abstr. 19. EGU2017-10478.
Masson-Delmotte, V., Schulz, M., Abe-Ouchi, A., Beer, J., Ganopolski, A., González Rouco, J.F., Jansen, E., Lambeck, K., Luterbacher, J., Naish, T., Osborn, T., Otto-Bliesner, B., Quinn, T., Ramesh, R., Rojas, M., Shao, X., Timmermann, A., Rouco, J.F.G., 2013. Information from paleoclimate Archives. In: Stocker, T.F., Qin, D., Plattner, G.K., Tignor, M., Allen, S.K., Boschung, J., Nauels, A., Xia, Y., Bex, V., Midgley, P.M. (Eds.), Climate Change 2013: the Physical Science Basis. Contribution of Working Group I to the Fifth Assessment Report of the Intergovernmental Panel on Climate Change. Cambridge University Press, Cambridge, U.K., pp. 383–464. http://dx.doi.org/10.1017/CBO9781107415324
Möller, P., Larsen, N.K., Kjær, K.H., Funder, S., Schomacker, A., Linge, H., Fabel, D., 2010. Early to middle Holocene valley glaciations on northernmost Greenland. Quat. Sci. Rev. 29, 3379–3398. http://dx.doi.org/10.1016/j.quascirev.2010.06.044.
Noël, B., van de Berg, W.J., Machguth, H., Lhermitte, S., Howat, I., Fettweis, X., van den Broeke, M.R., 2016. A daily, 1 km resolution data set of downscaled Greenland ice sheet surface mass balance (1958–2015). Cryosph 10, 2361–2377. http://dx.doi.org/10.5194/tc-10-2361-2016.
Nørgaard-Pedersen, N., Mikkelsen, N., Kristoffersen, Y., 2008. Late glacial and Holocene marine records from the independence Fjord and Wandel Sea regions, North Greenland. Polar Res. 27, 209–221. http://dx.doi.org/10.1111/j.1751-8369.2008.00065.x.
Nye, J.F., 1957. The distribution of stress and velocity in glaciers and ice-sheets. Proc. R. Soc. A Math. Phys. Eng. Sci. 239, 113–133. http://dx.doi.org/10.1098/rspa.1957.0026.
Olsen, J., Kjær, K.H., Funder, S., Larsen, N.K., Ludikova, A., 2012. High-Arctic climate conditions for the last 7000 years inferred from multi-proxy analysis of the Bliss Lake record, North Greenland. J. Quat. Sci. 27, 318–327. http://dx.doi.org/10.1002/jqs.1548.
Otto-Bliesner, B.L., Brady, E.C., Clauzet, G., Tomas, R., Levis, S., Kothavala, Z., 2006. Last glacial maximum and Holocene climate in CCSM3. J. Clim. 19, 2526–2544. http://dx.doi.org/10.1175/JCLI3748.1.
Overland, J.E., Wang, M., 2013. When will the summer Arctic be nearly sea ice free? Geophys. Res. Lett. 40, 2097–2101. http://dx.doi.org/10.1002/grl.50316.
Perren, B.B., Wolfe, A.P., Cooke, C.A., Kjær, K.H., Mazzucchi, D., Steig, E.J., 2012. Twentieth-century warming revives the world's northernmost lake. Geology 40, 1003–1006. http://dx.doi.org/10.1130/G33621.1.
Pollard, D., DeConto, R.M., 2009. Modelling West Antarctic ice sheet growth and collapse through the past five million years. Nature 458, 329–332. http://dx.doi.org/10.1038/nature07809.
Polyak, L., Alley, R.B., Andrews, J.T., Brigham-Grette, J., Cronin, T.M., Darby, D.A., Dyke, A.S., Fitzpatrick, J.J., Funder, S., Holland, M., Jennings, A.E., Miller, G.H., O'Regan, M., Savelle, J., Serreze, M., St. John, K., White, J.W.C., Wolff, E., 2010. History of sea ice in the Arctic. Quat. Sci. Rev. 29, 1757–1778. http://dx.doi.org/10.1016/j.quascirev.2010.02.010.
Reeh, N., 2004. Holocene climate and fjord glaciations in Northeast Greenland: implications for IRD deposition in the North Atlantic. Sediment. Geol. 165, 333–342. http://dx.doi.org/10.1016/j.sedgeo.2003.11.023.
Reeh, N., 1995. Report on Activities and Results 1993-1995 for Hans Tausen Ice Cap Project - Glacier and Climate Change Research, North Greenland. Report to the Nordic Minister Council.
Reeh, N., Mayer, C., Miller, H., Thomsen, H.H., Weidick, A., 1999. Present and past climate control on fjord glaciations in Greenland: implications for IRD-deposition in the sea. Geophys. Res. Lett. 26, 1039–1042. http://dx.doi.org/10.1029/1999GL900065.

Reeh, N., Olesen, O.B., Thomsen, H.H., Starzer, W., Bøggild, C.E., 2001. Mass balance parameterisation for Hans Tausen Iskappe, peary Land, Northern Greenland. Meddelelser Om. Grønl. Geosci. 39, 57–69.
Renssen, H., Seppä, H., Crosta, X., Goosse, H., Roche, D.M., 2012. Global characterization of the Holocene thermal maximum. Quat. Sci. Rev. 48, 7–19. http://dx.doi.org/10.1016/j.quascirev.2012.05.022.
Schweinsberg, A.D., Briner, J.P., Miller, G.H., Bennike, O., Thomas, E.K., 2017. Local glaciation in west Greenland linked to North Atlantic Ocean circulation during the Holocene. Geology 45, G38114.1. http://dx.doi.org/10.1130/G38114.1.
Simon, K.M., James, T.S., Dyke, A.S., 2015. A new glacial isostatic adjustment model of the Innuitian Ice Sheet, Arctic Canada. Quat. Sci. Rev. 119, 11–21. http://dx.doi.org/10.1016/j.quascirev.2015.04.007.
Sinclair, G., Carlson, A.E., Mix, A.C., Lecavalier, B.S., Milne, G., Mathias, A., Buizert, C., DeConto, R., 2016. Diachronous retreat of the Greenland ice sheet during the last deglaciation. Quat. Sci. Rev. 145, 243–258. http://dx.doi.org/10.1016/j.quascirev.2016.05.040.
Singarayer, J.S., Bamber, J.L., Valdes, P.J., 2006. Twenty-first-century climate impacts from a declining Arctic Sea ice cover. J. Clim. 19, 1109–1125. http://dx.doi.org/10.1175/JCLI3649.1.
Starzer, W., Reeh, N., 2001. Digital elevation models of the Hans Tausen ice cap. Meddeles. Om. Grønl. Geosci. 39, 45–56.
Steig, E.J., Huybers, K., Singh, H.A., Steiger, N.J., Ding, Q., Frierson, D.M.W., Popp, T., White, J.W.C., 2015. Influence of West Antarctic ice sheet collapse on Antarctic surface climate. Geophys. Res. Lett. 42, 4862–4868. http://dx.doi.org/10.1002/2015GL063861.
Thomsen, H.H., Reeh, N., Olesen, O.B., Jonsson, P., 1996. Glacier and climate research on Hans Tausen Iskappe, North Greenland - 1995 glacier basin activities and preliminary results. Grønl. Geol. Unders. 172, 78–84.
Vihma, T., 2014. Effects of Arctic Sea Ice Decline on Weather and Climate: a Review, Surveys in Geophysics. http://dx.doi.org/10.1007/s10712-014-9284-0.
Vinther, B.M., 2016. The RECAP ice core – recovering a full Glacial record from Eastern Greenland. Geophys. Res. Abstr. 18, EGU2016–10424.
Vinther, B.M., Buchardt, S.L., Clausen, H.B., Dahl-Jensen, D., Johnsen, S.J., Fisher, D.A., Koerner, R.M., Raynaud, D., Lipenkov, V., Andersen, K.K., Blunier, T., Rasmussen, S.O., Steffensen, J.P., Svensson, A.M., 2009. Holocene thinning of the Greenland ice sheet. Nature 461, 385–388. http://dx.doi.org/10.1038/nature08355.
Wake, L.M., Lecavalier, B.S., Bevis, M., 2016. Glacial isostatic adjustment (GIA) in Greenland: a review. Curr. Clim. Chang. Rep. 2, 101–111. http://dx.doi.org/10.1007/s40641-016-0040-z.
Weidick, A., 2001. Neoglacial glaciations around Hans Tausen Iskappe, peary Land, North Greenland. Meddelelser Om. Grønl. Geosci. 39, 5–26.
Zekollari, H., 2016. A MATLAB function for 3-D and 4-D topographical visualization in geosciences. Geophys. Res. Abstr. 18. EGU2016–3062.
Zekollari, H., Fürst, J.J., Huybrechts, P., 2014. Modelling the evolution of Vadret da Morteratsch, Switzerland, since the Little Ice Age and into the future. J. Glaciol. 60, 1208–1220. http://dx.doi.org/10.3189/2014JoG14J053.
Zekollari, H., Huybrechts, P., 2015. On the climate–geometry imbalance, response time and volume–area scaling of an alpine glacier: insights from a 3-D flow model applied to Vadret da Morteratsch, Switzerland. Ann. Glaciol. 56, 51–62. http://dx.doi.org/10.3189/2015AoG70A921.
Zekollari, H., Huybrechts, P., Fürst, J.J., Rybak, O., Eisen, O., 2013. Calibration of a higher-order 3-D ice-flow model of the Morteratsch glacier complex, Engadin, Switzerland. Ann. Glaciol. 54, 343–351. http://dx.doi.org/10.3189/2013AoG63A434.
Zekollari, H., Huybrechts, P., Noël, B., van de Berg, W.J., van den Broeke, M.R., 2017. Sensitivity, stability and future evolution of the world's northernmost ice cap, Hans Tausen Iskappe (Greenland). Cryosph 11, 805–825. http://dx.doi.org/10.5194/tc-11-805-2017.